

# Sintering and Properties of Silicon Nitride Densified with Liquids in the System MgO–AlN–SiO<sub>2</sub>

P. K. Das & J. Mukerji\*

Central Glass and Ceramic Research Institute, 196 Raja S C Mullick Road, Jadavpur, Calcutta–700 032, India

(Received 7 July 1987, revised version received 24 June 1988, accepted 5 July 1988)

## Abstract

Silicon nitride was pressureless sintered at 1700–1800°C with liquids in the ternary system MgO–AlN–SiO<sub>2</sub>, liquids rich in nitrogen and high MgO content sintered readily, Si<sub>3</sub>N<sub>4</sub> of 98% theoretical density was obtained. Heat treatments of the samples were carried out to crystallise the grain boundary phase. High-temperature flexural strength, fracture toughness and creep of the samples were measured. Increase in nitrogen content with constant MgO/SiO<sub>2</sub> ratio produced products with better thermomechanical properties. Superior products were obtained with high nitrogen and low MgO content in the sintering liquid due to a slower sintering rate and acicular grain growth. The best product had a flexural strength (4-point bending test, 40–20 mm) of 490 MPa and fracture toughness of 6.1 MPa m<sup>1/2</sup>. The creep strain rate and stress of a sample sintered with a liquid with a high MgO content were  $10 \times 10^{-5} \text{ h}^{-1}$  (at 1200°C) and 100 MPa, respectively.

Siliziumnitrid wurde drucklos zwischen 1700 und 1800°C mit einer Flussigphase des quasiternären Systems MgO–AlN–SiO<sub>2</sub> gesintert. Es wurden Dichten von 98%  $\rho_D$  erzielt, wobei Proben mit einer Flussigphase mit hohem Stickstoff- und MgO-Gehalten eine schnellere Verdichtung zeigten. Wärmebehandlungen wurden zur Auskristallisation der Korngrenzphasen durchgeführt. Außerdem wurden Hochtemperaturbiegefestigkeit, -bruchzähigkeit und -kriechen der Proben untersucht. Ein Anstieg des Stickstoffgehaltes bei konstantem MgO/SiO<sub>2</sub>-Verhältnis führte zu besseren thermomechanischen Eigenschaften. Die besten Produkte ergaben sich mit hohem Stickstoff- und geringen MgO-Gehalten in der

Flussigphase wegen der hierdurch verringerten Sinter-rate und dem stengelförmigen Kornwachstum. Die höchsten Festigkeiten (Auflager 40–20 mm) betragen 490 MPa und der  $K_{RC} = 6.1 \text{ MPa m}^{1/2}$ . Die Kriechdehnungsrate für eine gesinterte Probe mit hohem MgO-Gehalt betrug  $10 \times 10^{-5} \text{ h}^{-1}$  bei 1200°C und einer Belastung von 100 MPa.

Le nitride de silicium a été fritté naturellement entre 1700 et 1800°C en phase liquide dans le système ternaire MgO–AlN–SiO<sub>2</sub>, les liquides riches en azote et à haute teneur en MgO permettent un frittage plus rapide, on obtient une densité relative de 98%. Les échantillons ont été soumis à des traitements thermiques en vue de cristalliser la phase intergranulaire. La résistance à la flexion à haute température, la ténacité et la résistance au fluage des échantillons ont été mesurées. Une augmentation de la teneur en azote à taux MgO/SiO<sub>2</sub> constant améliore les propriétés thermomécaniques. De meilleurs produits ont été obtenus à l'aide d'un liquide à haute teneur en azote et faible teneur en magnésie, en raison d'une vitesse de frittage plus faible et d'une croissance anisotrope des grains. Le meilleur produit présente une résistance à la rupture en flexion (4 points, 40–20 mm) de 490 MPa et une ténacité de 6.1 MPa m<sup>1/2</sup>. La vitesse de fluage d'un échantillon fritté avec une phase liquide à haute teneur en magnésie est de  $10 \times 10^{-5} \text{ h}^{-1}$  à 1200°C sous une contrainte de 100 MPa.

## 1 Introduction

Early studies of sintering of Si<sub>3</sub>N<sub>4</sub> used MgO as a liquid forming agent<sup>1,2</sup>. This liquid, present at the grain boundaries, affects the high-temperature mechanical properties of sintered Si<sub>3</sub>N<sub>4</sub>, as, at high temperature,<sup>3</sup> it behaves like a viscous fluid.

\* To whom all correspondence should be addressed.

**Table 1.** Compositions of liquid sintering aids for sintering Si<sub>3</sub>N<sub>4</sub> (see also Fig 1)

Batch	Composition (wt% Si <sub>3</sub> N <sub>4</sub> + wt% liquid)	Addition (mol%)			Liquid composition	Composition (wt%) of N <sub>2</sub> in liquid
		MgO	AlN	SiO <sub>2</sub>		
P3	91Si <sub>3</sub> N <sub>4</sub> + 9M <sub>2</sub> S	100	—	—	Mg <sub>28.6</sub> Si <sub>14.3</sub> O <sub>57.2</sub>	nil
P4	77Si <sub>3</sub> N <sub>4</sub> + 23PG10	30.4	32.6	37	Mg <sub>12.8</sub> Si <sub>15.6</sub> Al <sub>13.8</sub> O <sub>44.0</sub> N <sub>13.8</sub>	9.57
P8	79Si <sub>3</sub> N <sub>4</sub> + 21PG8	10	40	50	Mg <sub>4.0</sub> Si <sub>20.0</sub> Al <sub>16.0</sub> O <sub>44.0</sub> N <sub>16.0</sub>	11.10
P12	79Si <sub>3</sub> N <sub>4</sub> + 21PG1	27	40.2	32.8	Mg <sub>11.6</sub> Si <sub>14.1</sub> Al <sub>17.3</sub> O <sub>39.3</sub> N <sub>17.3</sub>	11.97

Terwilliger and Lange<sup>4</sup> presented a model of pressureless sintering of Si<sub>3</sub>N<sub>4</sub> with 5% MgO, showing that pore growth due to decomposition causes a decrease in the driving force for sintering with consequent stoppage of shrinkage. Several other oxides of Y, Ce, Zr, La and Sm have been tried later as sintering aids to improve the thermomechanical properties of the product.<sup>5-12</sup> Post-sintering heat treatment reduces the amount of glassy phase as it precipitates a refractory phase at the grain boundaries. This improves the high temperature properties. Giachello *et al.*,<sup>13</sup> using 8% Y<sub>2</sub>O<sub>3</sub> and 1% MgO as sintering aid, obtained a 44% increase in strength at 1125°C upon devitrification. Work on other liquid sintering systems, viz Y<sub>2</sub>O<sub>3</sub>-AlN-SiO<sub>2</sub><sup>14,15</sup> and Ce<sub>2</sub>O<sub>3</sub>-AlN-SiO<sub>2</sub>,<sup>16</sup> also showed improvement in strength and fracture toughness of pressureless sintered Si<sub>3</sub>N<sub>4</sub> upon post-sintering heat treatment. Tsuge and co-workers,<sup>17,18</sup> using Y<sub>2</sub>O<sub>3</sub> and (Y<sub>2</sub>O<sub>3</sub> + Al<sub>2</sub>O<sub>3</sub>), obtained yttrium aluminium garnet (YAG) as a grain boundary crystalline phase only when Y<sub>2</sub>O<sub>3</sub>/Al<sub>2</sub>O<sub>3</sub> ≥ 2, which improved the mechanical properties. Masaki and Kamigaito<sup>19</sup> sintered Si<sub>3</sub>N<sub>4</sub> with MgO, Al<sub>2</sub>O<sub>3</sub> and spinel separately, and observed that the best sintering and strength was achieved with a mixture of MgO, Al<sub>2</sub>O<sub>3</sub> and spinel. In a similar attempt, Rabinovich *et al.*<sup>20</sup> obtained the best sintering (95%) and MOR (350-400 MPa) with 15% spinel. The grain boundary phase was either a glass or a Mg-Al-spinel. Sintering of Si<sub>3</sub>N<sub>4</sub> with a nitrogen-rich liquid phase has been studied<sup>21,22</sup> to increase the viscosity of the grain boundary glassy phase at high temperature and to precipitate out Si<sub>3</sub>N<sub>4</sub> and other crystalline phases from the liquid on reaction or by a post-sintering heat treatment.

This paper deals with the pressureless sintering of Si<sub>3</sub>N<sub>4</sub> with liquids selected from the system MgO-AlN-SiO<sub>2</sub>. The formation of glasses and melts in this system and their behaviour is discussed. AlN was selected as one of the raw material to introduce N<sub>2</sub> into the system to take advantage of the reaction<sup>23</sup>



The MgO-SiO<sub>2</sub>-Al<sub>2</sub>O<sub>3</sub> phase diagram indicates

that MgAl<sub>2</sub>O<sub>4</sub> (m.p. 2138°C) spinel may form by further reaction of Al<sub>2</sub>O<sub>3</sub> with the MgO in the batch



Two principles were followed in selecting the composition of the liquid: (a) the composition should be away from the region where complete vitrification occurs and (b) the composition should lie around the line MgO-(4AlN-3SiO<sub>2</sub>) in order to precipitate out MgAl<sub>2</sub>O<sub>4</sub> either during sintering or upon post-sintering heat treatment. Only one composition of the externally added sintering aid had the molar ratio corresponding to forsterite (2MgO-SiO<sub>2</sub>) (see Composition 1, Table 1 and Fig 1). The aim of the present work is to densify Si<sub>3</sub>N<sub>4</sub> with a predetermined nitrogen-rich liquid composition which devitrifies easily, forming refractory crystalline products. The sintering behaviour and thermomechanical properties, both of the as-sintered and heat-treated samples, are reported.

## 2 Experimental Procedure

Laboratory-prepared Si<sub>3</sub>N<sub>4</sub> having (%) N, 38.63 ± 0.52, O, 2.2 ± 0.3, Ca, 0.053, Mg, 0.01, Na, 0.084, Fe, 0.138, α-Si<sub>3</sub>N<sub>4</sub>, 86, and surface area 8.78 m<sup>2</sup> g<sup>-1</sup> was used. The other raw materials were MgO (E. Merck, Darmstadt, FRG, >97% Fe, 0.005, Ca, 0.3, Na, 0.2, K, 0.005%), AlN (Starck 'A', Goslar, FRG, C, 0.05, Fe, 0.1, Al, 65.5, N, 32.5%) and SiO<sub>2</sub> (Hesla Mineral, Ranchi, India, optical grade, >99.9% Fe<sub>2</sub>O<sub>3</sub>, 0.004%). Different liquid sintering aid compositions are given in Table 1 and Fig 1. The surface SiO<sub>2</sub> (4.1 wt%) in Si<sub>3</sub>N<sub>4</sub> was taken into account during preparation of the batch composition. The components were weighed to ±0.01 g, and 100 g of the batches were attrited in *n*-hexane using alumina balls and pot. Alumina pick-up in each grinding of 3 h was about 0.5 wt%. The powder was sieved through a 200-mesh sieve and dried. For the sintering study, cylindrical pellets of dimension 15.5 mm diameter × 14.5 mm height were prepared at 200 MPa isostatic pressure. Sintering studies were generally done at 1700°C for 20 min with an average temperature rise of about 30°C min<sup>-1</sup>. Temperature

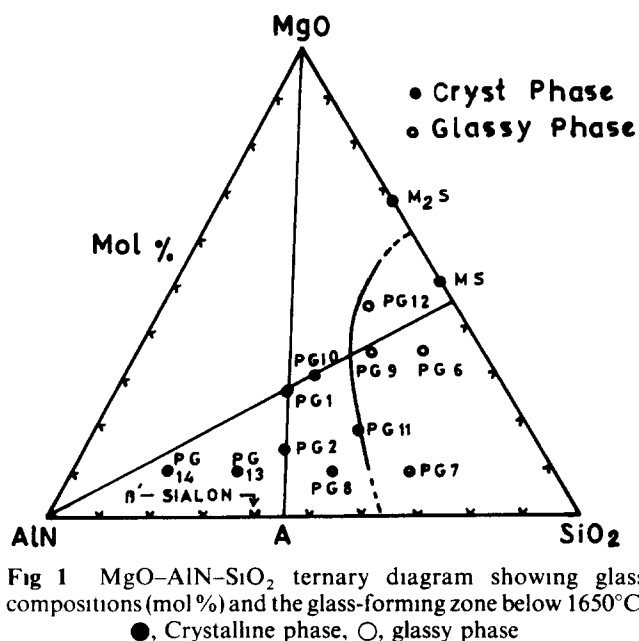


Fig 1 MgO-AlN-SiO<sub>2</sub> ternary diagram showing glass compositions (mol %) and the glass-forming zone below 1650°C  
●, Crystalline phase, ○, glassy phase

and shrinkage were plotted by a two-pen X-Y recorder. For other studies, bars of size 67 mm × 17 mm × 15 mm were prepared from the green powder at different isostatic pressures. They were fired at 1700–1800°C for 30–60 min to obtain better densification. Sintering was carried out in a graphite resistance-heated furnace in a BN-coated graphite crucible using a packing of Si<sub>3</sub>N<sub>4</sub> powder in a pure nitrogen atmosphere. Details of the preparation are given in Table 2. The change in dimensions was measured up to 0.01 mm and densities by the water immersion method. Crystallisation of the samples was generally carried out at 1330°C in pure nitrogen for 24 h. The phases present in uncrystallised and crystallised samples were determined by XRD using a Cu<sub>Kα</sub> target.

Measurement of the strength of the samples was done by 4-point bending using 40 mm total span and 20 mm constant bending moment span (40 mm–20 mm). Bars of size 45 mm × 4.5 mm × 3.5 mm were ground to 600-mesh emery powder and then polished with 2 μm diamond paste. The loading rate was 1.25 N s<sup>-1</sup>. Fracture toughness ( $K_{Ic}$ ) was measured with the same bars by the single edge notched bend technique. Notch thickness was generally 0.2 mm and  $a/w$  varied from 0.2 to 0.65 with notch radius  $R$  values from 0.25 to 0.4 mm, where  $a$  is the notch length and  $w$  is the sample width.

Measurement of creep strain rate ( $\dot{\epsilon}$ ) of the samples P3 and P4 was done under flexure with test bars of the same dimensions as in the MOR measurement. The temperature and stress were varied from 1100 to 1300°C and 75 to 300 MPa, respectively.

### 3 Results and Discussion

#### 3.1 Sintering

The glass-forming zone in the MgO-AlN-SiO<sub>2</sub> system is shown in Fig 1. The zone close to SiO<sub>2</sub>, viz PG6, PG9 and PG12, forms clear and complete glasses but this tendency decreases as the amount of nitrogen in the glass composition in terms of AlN increases.<sup>24</sup> The curved line separates the zone of compositions which, when cooled, formed complete glasses at 1650°C from those which did not. The compositions in the zone to the left of the line generally yielded different crystalline phases in the melt, depending upon composition. The melting point also increased with the nitrogen content of the compositions. Thus, as the composition approached

Table 2. Observations made during sintering of silicon nitride

Batch	Average surface area (m <sup>2</sup> g <sup>-1</sup> )	Isostatic pressure (MPa)	Sintering temperature (°C)	Sintering time (min)	Linear shrinkage (%)	Evaporation loss (%)	Fired density (Mg m <sup>-3</sup> )	Phases	
								As-sintered	Crystallised
P3	12.51	95	1700	40	20.70	4.61	3.03	β-Si <sub>3</sub> N <sub>4</sub>	β-Si <sub>3</sub> N <sub>4</sub> , Si <sub>2</sub> N <sub>2</sub> O
		285	1700	40	19.42	0.91	3.12		
P4	10.46	143	1650	60	18.05	5.16	3.02	β-Si <sub>3</sub> N <sub>4</sub>	β-Si <sub>3</sub> N <sub>4</sub> , Si <sub>2</sub> N <sub>2</sub> O
		143	1700	60	19.18	1.40	3.13		
		143	1750	60	19.68	2.57	3.07		
		143	1800	60	18.00	3.82	2.98		
		429	1700	60	13.75	2.07	3.02		
P8	14.30	285	1800	30	17.58	2.74	3.06	β-Si <sub>3</sub> N <sub>4</sub>	β-Si <sub>3</sub> N <sub>4</sub> , Si <sub>2</sub> N <sub>2</sub> O (tr), other (tr)
P12	10.68	285	1750	60	13.28	21.22	2.87	β-Si <sub>3</sub> N <sub>4</sub>	β-Si <sub>3</sub> N <sub>4</sub> , Si <sub>2</sub> N <sub>2</sub> O, MgAl <sub>2</sub> O <sub>4</sub> , other
		285	1800	30	16.32	1.51	3.10		

The diffractogram of the as-sintered sample when compared with the KCl showed a slight shift of the 200 peak of β-Si<sub>3</sub>N<sub>4</sub>, whereas for the other two peaks (101 and 210) the shifts were irregular. It was therefore assumed if there was any formation of solid solution of Si<sub>3</sub>N<sub>4</sub> with alumina to form sialon the amount of substitution would be very low.

the AlN corner, a more refractory grain boundary phase was expected to form. Compositions PG13 and PG14 did not melt at all, even at 1750°C, due to the high AlN content. Compositions for liquid sintering aids were selected from outside the complete glass-forming zone which could yield crystallised grain boundary phases during cooling after sintering or upon heat treatment. The composition of liquid sintering aids is expected to alter very little at high temperature as the dissolution of  $\text{Si}_3\text{N}_4$  would be low in a nitrogen-rich liquid. The compositions are tabulated in Table 2.

The dynamic sintering data of the P4 and P12 compositions are plotted in Fig 2(a) and (b). A small shrinkage of 1% was observed at 1110°C with the P12 composition. Thereafter the sintering of particles increased, the maximum rate of which was 4.63 and 5.1  $\text{min}^{-1}$  at 1592 and 1640°C for P4 and P12, respectively. The higher percentage of liquid in P4 (23 wt%) was probably responsible for the higher reaction rate as observed from the peak heights of P12, as compared with P4, which contained 21 wt% liquid. At this stage, the shrinkage may be attributed to both a particle rearrangement and a solution reprecipitation mechanism. The shift of maximum sintering rate for P12 to 1640°C was probably due to the higher nitrogen content of the composition with consequent higher viscosity.

The sintering of samples was performed for different periods at fixed temperatures (Table 2). For P3 the sintering additive corresponded to the composition of forsterite ( $\text{M}_2\text{S}$ ). The melt formed with this composition can sinter  $\text{Si}_3\text{N}_4$  well at 1700°C in 40 min. The fired density was 3.12  $\text{g cm}^{-3}$ , which was almost 98% that of  $\text{Si}_3\text{N}_4$ . The maximum density obtained by Terwilliger and Lange using 5 wt% MgO was 86% of the theoretical at 1570°C after 46 min without pressure<sup>4</sup> and almost theoretical after 4 h at 1650°C with pressure<sup>1</sup>. Densification occurs, according to them, by rapid rearrangement of grains upon formation of the eutectic liquid which has a very low contact angle of only 5°. With the liquid composition PG10, 98% densification was achieved at 1700°C in 1 h. This liquid composition contained relatively high amounts of MgO and  $\text{SiO}_2$ , and a lower amount of AlN. The effect of high temperature (1750–1800°C) on consolidation was deleterious due to decomposition of the nitrogen-containing liquid. At lower temperature (1650°C) the amount of liquid phase was not large enough to sinter the product to its full density. At 1700°C the liquid can produce 95% densification within 3 min. The composition of PG8 had a higher amount of AlN (40 mol%) and a lower

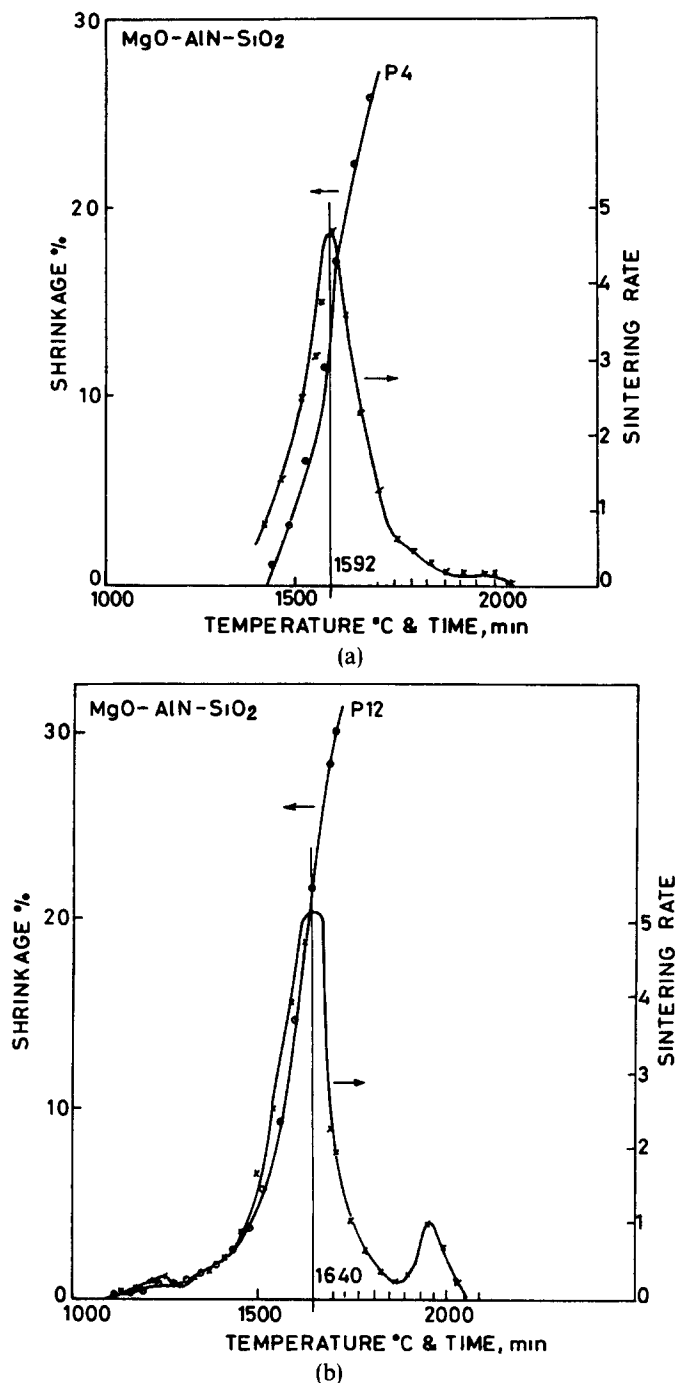


Fig. 2. Dynamic sintering study of (a) P4 and (b) P12 compositions. One small division on x-axis represents 2 min.

amount of MgO (10 mol%). This liquid could produce an approximately 96% dense material in 30 min at 1800°C. PG1, containing the same amount of AlN as PG8 but having a higher MgO (27 mol%) and a lower  $\text{SiO}_2$  (32.8 mol%) content, could sinter P12 to 97% of the theoretical density under the same conditions.

### 3.2 Phases obtained after crystallisation

The initial crystallisation trial carried out at 1200, 1330 and 1400°C for 24 h in pure nitrogen showed

that the best temperature for crystallisation was 1330°C. Crystallisation products obtained are shown in Table 2. The composition P3 yielded only  $\text{Si}_2\text{N}_2\text{O}$  on crystallisation. On crystallisation the compositions P4 and P12 produced another phase with  $d$  values of 3.55 and 3.50 Å in addition to  $\text{Si}_2\text{N}_2\text{O}$ . It may be noted that the liquid of composition P12 lying on the MgO–Al join of Fig. 1 is close to P4 which contains liquid PG10. In addition, a small amount of Mg–Al-spinel was observed in the crystallised product of P12. It may be noted further that in most of the cases Mg-containing crystalline phases did not precipitate, indicating that Mg remained in the nitrogen glasses where it acts as a network former. The P8 composition yielded a very small amount of  $\text{Si}_2\text{N}_2\text{O}$  and some unidentified phases with  $d$  values of 4.040, 3.121 and 2.304 Å. Although the liquid content was 23 wt% the peak heights were very small, indicating that the amount of crystalline phase precipitated was small. This composition lies towards the  $\text{SiO}_2$  corner with low Mg content and the glass is expected to be more stable. The observation suggests that for easy crystallisation of the grain boundary liquid the composition should be selected from the left side of the MgO–Al join (Fig. 1).

### 3.3 Microstructure

The microstructure was examined by SEM after etching polished surfaces with NaOH at 350°C for 30 s. Polishing was done initially up to 600-mesh emery powder and finally with 2 µm diamond paste on a polishing disc. Figures 3, 4 and 5 show the microstructures of P3, P4 and P8 samples, respectively. The grains in P3 and P8 are generally elongated, with P8 having the higher aspect ratio, the grains in P4 are more equiaxed. P4 and P8 contained 23 and 21 wt% liquids, respectively. This

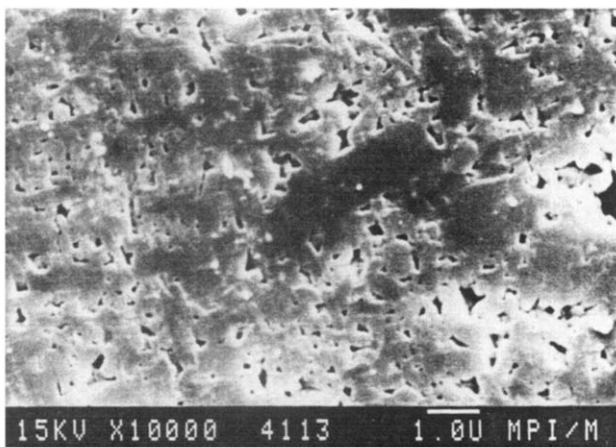


Fig. 3. Microstructure of P3 sample

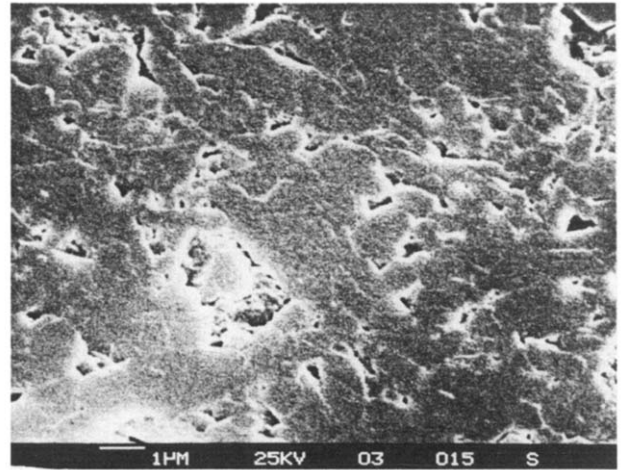


Fig. 4. Microstructure of P4 sample

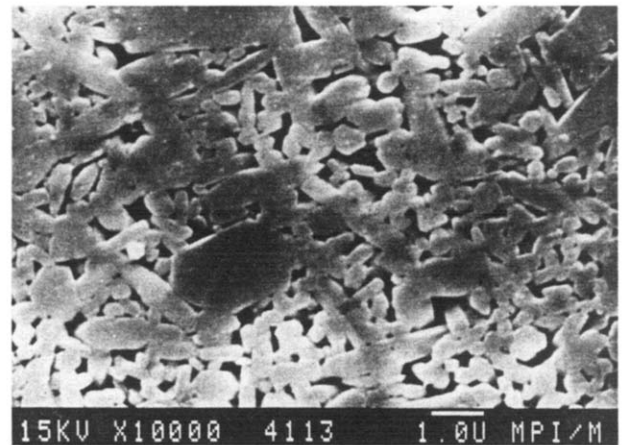


Fig. 5. Microstructure of P8 sample

is reflected in Figs 4 and 5. The distribution of the liquid is found to be even in the P8 sample.

## 4. Mechanical Properties

### 4.1 Flexural strength

The flexural strength of sintered samples is shown in Fig. 6. The P3 sample sintered with the liquid on the MgO– $\text{SiO}_2$  binary and not containing nitrogen showed a low strength of 300 MPa. The flexural strength of the samples increased as nitrogen was introduced in the sintering liquid. The P4 and P12 samples had almost the same MgO– $\text{SiO}_2$  ratio but the amount of nitrogen in the sintering liquids was 13.8 and 17.3 atom%, respectively. Both showed higher strength than P3. P12, having a higher nitrogen content, was superior to P4 in strength. Low MgO content and the presence of nitrogen both make the liquid less reactive. A slow solution reprecipitation favours preferential growth in the  $c$ -direction. Such liquid will be also more viscous than

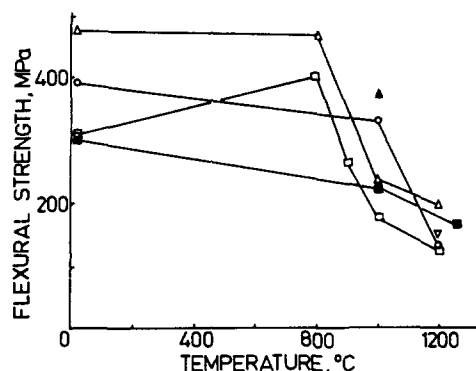


Fig. 6. Variation of flexural strength of  $\nabla$ , P3,  $\square$ , P4,  $\blacksquare$ , P4 crystallised,  $\triangle$ , P8,  $\blacktriangle$ , P8 crystallised, and  $\circ$ , P12 samples with temperature

that of P4 and P12 because of the presence of a high amount of nitrogen and  $\text{SiO}_2$ . As a result P8 could not be sintered to full density in a short time at  $1750^\circ\text{C}$  like the other compositions but required  $1800^\circ\text{C}$ . The microstructure of P8 showed preferential growth in the  $c$ -direction, giving rise to an interwoven acicular microstructure which resulted in superior mechanical properties. In contrast, the microstructure of the samples containing a liquid with a higher  $\text{MgO}/\text{SiO}_2$  ratio with or without nitrogen, such as P3 and P4, showed relatively equiaxed grains with consequent lower strength and toughness. Liquids with a high  $\text{MgO}$  content had high reactivity, for example, P4 could be sintered to over 95% density in 3 min at  $1700^\circ\text{C}$ .

Composition P12 had almost the same  $\text{MgO}/\text{SiO}_2$  ratio but higher nitrogen content than P4 and was superior to it both at room temperature and at high temperature in flexural strength. This composition also lay on the  $\text{MgO}$ -A join (Fig 1), where  $\text{Mg}$ -aluminate ( $\text{MgO}-\text{Al}_2\text{O}_3$ ) was expected to form. After crystallisation P4 and P8 showed 33 and 29% improvement in flexural strength, respectively, at  $1000^\circ\text{C}$  (Table 3).

The rate of decrease of MOR above  $800^\circ\text{C}$  for P4 and P8 was lower above  $1000^\circ\text{C}$ , probably because of devitrification of the grain boundary phase occurring during testing above  $1000^\circ\text{C}$ .

#### 4.2 Fracture toughness

The fracture toughness ( $K_{\text{IC}}$ ) of three compositions is plotted in Fig 7, both at room temperature and at higher temperatures. Room-temperature fracture toughness values of the compositions were dependent upon the nitrogen content of the glassy sintering aid, which increases the hardness of the grain boundary glass<sup>25,26</sup>. The value of  $K_{\text{IC}}$  was low in the case of the P3 sample, probably due to the absence of nitrogen.  $K_{\text{IC}}$  values increased as the amount of nitrogen in the grain boundary glass of the samples

Table 3. Flexural strength of uncrystallised and crystallised samples

Sample	Flexural strength ( $\sigma$ ) (MPa)		$\frac{\sigma_{1000}}{\sigma_{\text{RT}}}$
	Room temperature (15–20°C)	1000°C	
P4	330	177	0.41
P4 crystallised	300	223	0.74
P8	487	240	0.49
P8 crystallised	483	380	0.78

was increased. The value of  $K_{\text{IC}}$  at higher temperature fell drastically in the P4 sample, and was also greatly reduced for P3 and P8 samples. The highest fracture toughness obtained was  $6.1 \text{ MPa m}^{1/2}$  for sample P8, which is comparable ( $6.0 \text{ MPa m}^{1/2}$ )<sup>15</sup> to that of a sample sintered with a liquid in the  $\text{Y}_2\text{O}_3$ - $\text{AlN}$ - $\text{SiO}_2$  system having an almost similar molar composition in glass but with 11 wt% liquid content. The reasons are discussed in the previous section. Fracture toughness of crystallised P4 showed a lower value than the original sample at room temperature but exceeded the value of the uncrystallised sample at about  $900^\circ\text{C}$  and remained higher above this temperature. Variation of  $K_{\text{IC}}$  of crystallised P4 was also much less than for uncrystallised P4. Thus the good effect of grain boundary crystallisation was established. The value of  $K_{\text{IC}}$  for the P8 sample was  $5.3 \text{ MPa m}^{1/2}$  at  $1200^\circ\text{C}$ , due to the high nitrogen content of the grain boundary glass which is itself tough<sup>25</sup>.

At and above  $1000^\circ\text{C}$ , the stress-strain behaviour of the P3 and P4 samples was also non-linear. This type of non-linearity was an indication of plastic flow which ultimately leads to the occurrence of slow crack growth<sup>27</sup>.

#### 4.3 Creep

Creep data for the P3 and P4 samples are tabulated in Table 4 and plotted in Fig 8. The samples were

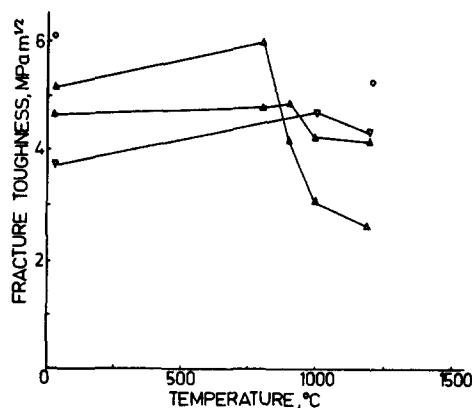


Fig. 7. Variation of fracture toughness of  $\nabla$ , P3,  $\triangle$ , P4,  $\blacktriangle$ , P4 crystallised, and  $\circ$ , P8 samples with temperature

**Table 4** Data on creep behaviour of P3 and P4 samples

Composition	Temperature (°C)	Stress (MPa)	Duration (h)	Creep strain rate ( $h^{-1} \times 10^{-6}$ )	Steady-state creep strain ( $h^{-1} \times 10^{-6}$ )	n	Activation energy ( $kJ mol^{-1}$ )
P3	1150	75	10	0.2	0.2	3.0	303
		1200	57	0.45	0.45		
	1200	200	40	0.5	0.5	2.4	
		300	53	3.3	2.2		
	1300	100	92	2.1	0.79	2.4	
		150	78	3.0	2.1		
1300	200	96	8.1	4.0			
P4	1100	75	28	1.8	1.8	311	
	1150	75	20	4.2	4.2		
	1200	75	20	10	10		

tested between 1100 and 1300°C at loads varying between 75 and 300 MPa. The values of the stress exponent ( $n$ ) obtained for P3 was 3 at 1200°C and 2.4 at 1300°C. As these values were far from 1, the creep may be controlled by non-Newtonian flow of liquid at the grain boundaries. Activation energies of the P3 and P4 compositions calculated from an Arrhenius plot (Fig. 9) were 303 kJ mol<sup>-1</sup> at 200 MPa in the temperature range 1150–1300°C and 312 kJ mol<sup>-1</sup> at 75 MPa between 1100–1200°C, which are similar to those quoted in the literature<sup>28,29</sup>

## 5 Conclusions

(a) Densification of Si<sub>3</sub>N<sub>4</sub> to over 98% theoretical density was achieved with a liquid composition selected from outside the glass-forming region in the system MgO–AlN–SiO<sub>2</sub>.

(b) The refractory MgAl<sub>2</sub>O<sub>4</sub> phase could be crystallised out from the grain boundary glass of sintered Si<sub>3</sub>N<sub>4</sub> (P12) when the liquid composition (PG1) lay on the tie-line MgO–(4 AlN 3 SiO<sub>2</sub>). In other cases Si<sub>2</sub>N<sub>2</sub>O was the phase crystallising out during heat treatment.

(c) Liquids in the system MgO–AlN–SiO<sub>2</sub> having

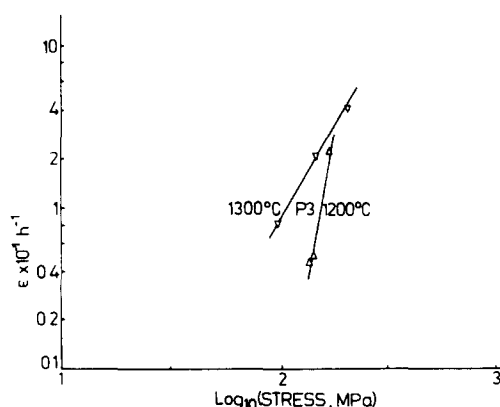


**Fig. 8** Variation of steady-state creep strain rate ( $\epsilon$ ) of stress

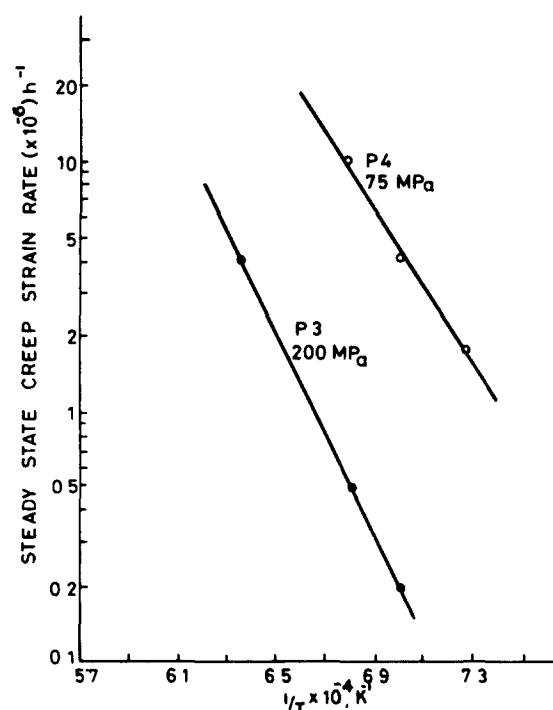


**Fig. 9.** Activation energy for creep of P3 and P4 samples

less than 10 mol% MgO and greater than 40 mol% AlN produced sintered products (P8) with good mechanical properties at high temperature.

(d) Liquids containing around 30 mol% MgO (PG10) were very reactive and could sinter Si<sub>3</sub>N<sub>4</sub> to over 95% of the theoretical density in 3 min at 1700°C. However, the sintering range appears to be very small.

(e) Heat treatment resulted in an improvement in strength at 1100°C as high as 33%.

## Acknowledgements

The authors are grateful to the Aeronautical Research and Development Board, Ministry of Defence, Government of India, for financial grant.

No 296 and for their permission to publish the paper Thanks are also due to colleagues for experimental assistance

## References

- 1 Terwilliger, G R & Lange, F F, Hot pressing behaviour of  $\text{Si}_3\text{N}_4$  *J Amer Ceram Soc*, **57**(1) (1974) 25–9
- 2 Jack, K H, Sialon glasses In *Nitrogen Ceramics*, ed F L Riley Nordhoff-Leyden, Amsterdam, 1977, p 257
- 3 Clarke, D R & Thomas, G, Grain boundary phases in hot pressed MgO fluxed  $\text{Si}_3\text{N}_4$  *J Amer Ceram Soc*, **60**(11–12) (1977) 491–5
- 4 Terwilliger, G R & Lange, F F, Pressureless sintering of  $\text{Si}_3\text{N}_4$  *J Mater Sci*, **10** (1975) 1169–74
- 5 Sanders, W A & Mieskowski, D M, Strength and microstructure of sintered  $\text{Si}_3\text{N}_4$  with rare earth additions *Amer Ceram Soc Bull*, **64**(2) (1985) 304–8
- 6 McDonough, W, Freiman, S W, Rice, R W & Becher, P F, Preliminary strength tests of silicon nitride hot pressed with  $\text{ZrO}_2$  or  $\text{ZrSiO}_4$  additions In *Proc DARPA/NAVSEA Ceramic Gas Turbine Demonstration Engine Program MCIC Report*, Batelle Columbus Laboratories, Columbus, Ohio, 1978, pp 625–7
- 7 Mitomo, M, The sintering of  $\text{Si}_3\text{N}_4$  under high nitrogen pressure In *Proc of Int Symp on Factor of Densification and Sintering of Oxide and Non-oxide Ceramics*, Japan, 1978, pp 539–44
- 8 Mah, T L, Mazdiyasi, K S & Ruh, R, The role of cerium orthosilicate in the densification of  $\text{Si}_3\text{N}_4$  *J Amer Ceram Soc*, **62**(1–2) (1979) 12–16
- 9 Galasso, F G & Veltri, R, Sintering of  $\text{Si}_3\text{N}_4$   $15\text{Y}_2\text{O}_3$  under high nitrogen pressure *Amer Ceram Soc Bull*, **58**(8) (1979) 793–4
- 10 Loehman, R E & Rowcliffe, D J, Sintering of  $\text{Si}_3\text{N}_4$ – $\text{Y}_2\text{O}_3$ – $\text{Al}_2\text{O}_3$  *J Amer Ceram Soc*, **63**(3–4) (1980) 144–8
- 11 Woting, G, Pertzsch, R & Hausner, H, Investigation of sintering of silicon nitride by dilatometry under high nitrogen pressure *Sci Sintering*, **17**(1/2) (1985) 87–95
- 12 Tani, E, Umabayashi, S, Kishi, K & Nishijima, M, Gas pressure sintering of  $\text{Si}_3\text{N}_4$  with concurrent addition of  $\text{Al}_2\text{O}_3$  and 5% rare earth oxides, high fracture toughness with fibre like structure *Amer Ceram Soc Bull*, **65**(9) (1986) 1131–51
- 13 Giachello, A, Martinengo, P C, Tommasini, G & Popper, P, Sintering and properties of  $\text{Si}_3\text{N}_4$  containing  $\text{Y}_2\text{O}_3$  and MgO *Amer Ceram Soc Bull*, **59**(12) (1980) 1212–15
- 14 Mukerji, J, Greil, P & Petzow, G, Sintering of  $\text{Si}_3\text{N}_4$  with nitrogen-rich liquid phase *Sci Sintering*, **15**(1) (1983) 43–53
- 15 Das, P K & Mukerji, J, Sintering behaviour and properties of  $\text{Si}_3\text{N}_4$  sintered with nitrogen-rich liquid in the  $\text{Y}_2\text{O}_3$ – $\text{AlN}$ – $\text{SiO}_2$  system *Amer Ceram Soc, Adv Ceram Mat*, **3**(3) (1988) 234–43
- 16 Mukerji, J, Das, P K, Greil, P & Petzow, G, Sintering  $\text{Si}_3\text{N}_4$  with liquid in the system  $\text{Ce}_2\text{O}_3$ – $\text{AlN}$ – $\text{SiO}_2$  *Ceram Int*, **13**(4) (1987) 215–21
- 17 Tsuge, A, Nishida, K & Komatsu, M, Effect of crystallising the grain boundary glass phase on the high temperature strength of hot pressed  $\text{Si}_3\text{N}_4$  containing  $\text{Y}_2\text{O}_3$  *J Amer Ceram Soc*, **58**(7–8) (1975) 323–6
- 18 Tsuge, A & Nishida, K, High strength and pressed  $\text{Si}_3\text{N}_4$  with concurrent  $\text{Y}_2\text{O}_3$  and  $\text{Al}_2\text{O}_3$  additions *Amer Ceram Soc Bull*, **57**(4) (1978) 424–6
- 19 Masaki, H & Kamigaito, O, Pressureless sintering of  $\text{Si}_3\text{N}_4$  with addition of MgO  $\text{Al}_2\text{O}_3$  and/or spinel *Yogyo Kyokai Shi*, **84**(10) (1976) 508–12
- 20 Rabinovich, E, Harel, L & Fischer, R, Pressureless sintering of  $\text{Si}_3\text{N}_4$  with spinel admixture *Proc Brit Ceram Soc, Sp Ceramics*, No 31 (1981) 71–84
- 21 Das, P K & Mukerji, J, Dense  $\text{Si}_3\text{N}_4$  by liquid phase sintering *Ind J Technol*, **24** (1986) 209–14
- 22 Das, P K & Mukerji, J, Sintering of  $\text{Si}_3\text{N}_4$  with liquids in the system MgO– $\text{AlN}$ – $\text{SiO}_2$  In *Collected papers, Proc World Cong on High Tech Materials, 6th CIMTEC*, Milano, 1986, pp 953–9
- 23 Torre, J P & Mocellin, M, Reactions chimiques entre la silice et le nitrure d'aluminium *Compt Rendus Acad Sci (Paris), Serie C*, **27**(9) (1974) 943–6
- 24 Das, P K & Mukerji, J, Nitrogen glass in the system MgO– $\text{AlN}$ – $\text{SiO}_2$  In *Collected papers, XIV Int Congr on Glass*, New Delhi, 1986, pp 104–9
- 25 Mukerji, J, Das, P K & Chakraborty, D, Properties of glasses and melts in the system MgO– $\text{AlN}$ – $\text{SiO}_2$  *Amer Ceram Soc Bull*, **66**(11) (1987) 1416–19
- 26 Loehman, R E, Preparation and properties of Y–Si–Al–O–N glasses *J Amer Ceram Soc*, **62**(1–10) (1979) 491–4
- 27 Mukerji, J, Das, P K, Rakshit, J & Bandopadhyay, S, Final Report on ARDB Defence Grant-in-Aid Project, Grant No AERO/RD 134/100/10/81-82/296, C G & C R I, Calcutta, India, Pt 2, Vol Two, March 1987, pp 27–56
- 28 Salah Ud Din & Nicholson, P S, Creep of hot pressed  $\text{Si}_3\text{N}_4$  *J Mater Sci*, **10**(7) (1975) 1375–80
- 29 Steinmann, D & Gugel, D, Dichtes Siliziumnitrid mit guten Hochtemperatureigenschaften und hohem Oxidationswiderstand In *Science of Ceramics, No 11*, ed R Carlsson & S Carlsson Swedish Ceram Soc, 1981, pp 113–21